

OPTIMAL 3D QUADRUPOLE SHAPES*

R. Baartman, TRIUMF, 4004 Wesbrook Mall, Vancouver, BC, V6T 2A3, Canada

Abstract

The usual practice of constructing quadrupoles from truncated cylindrical hyperbolae is put into question. A new shape is proposed. This shape has an analytic potential function. The exact shape of the analytic quadrupole may be impractical, but in the short case where aspect ratio ≈ 1 , pole shapes can be spherical. The optimal spherical radius is found to be 1.54 times the aperture radius. An example is also given demonstrating that in the long quad limit, the aberrations of order 5 and higher are much lower for the optimized shape.

A somewhat extended version of this paper has been published previously [1].

INTRODUCTION

The multipole elements commonly used to control charged particle beams correspond to solution terms of the Laplace equation $\nabla^2 V = 0$, namely, in polar coordinates (r, θ) , $r^n \cos n\theta$ in the system where the potential on axis is zero. Thus $n = 2$ for a quadrupole, 3 for a sextupole, etc. This implicitly assumes the elements are infinitely extended in the axial (z) direction, and of course in real beamlines, they are not. For $n = 2$, the intended linear dependence of the fields upon transverse coordinate is thus broken by the finiteness of the quadrupole. This results in nonlinear force terms and aberrations.

It is not obvious how to axially terminate the poles of a quadrupole. Often, they are simply truncated. Does the shape in the longitudinal direction matter? And if so, what shape is optimal? For very long quadrupoles, it can be argued that hyperbolic equipotential surfaces given by $r^2 \cos 2\theta = \text{constant}$ are optimal. However, this is only true sufficiently far from the ends; for quadrupoles whose length is comparable to or shorter than the aperture, the 2-D hyperbolic shape is clearly not optimal. What then is the optimal shape of quadrupoles in the short limit? What is the optimal shape in the long limit? Answering these questions is the subject of this paper.

Hardness of the Fringe Field

In the limit where the fringe field extent is short compared with the focal length of the quadrupole, the lowest order aberration (cubic force) effect is independent of fringe field shape. This was shown in 1997 [2].

Let the strength function of the quadrupole be $k(z)$. Rigorously, this means $\partial_{xx}V = -\partial_{yy}V = k(z)$ along the axis $x = y = 0$, so that

$$V(x, y, z) \rightarrow \frac{k(z)}{2}(x^2 - y^2) \text{ as } (x, y) \rightarrow (0, 0), \quad (1)$$

* TRIUMF receives federal funding via a contribution agreement through the National Research Council of Canada.

In the ‘‘hard-edge’’ limit, k is a step function. But using a discontinuous step function instead of an analytic function to calculate the optics leads to dramatically incorrect results. It is thus regrettable that almost all the major higher order optics codes allow calculation of third order optics in the ‘‘no fringe field’’ case. This case is unphysical because it brings a particle from the field-free region outside the quadrupole instantaneously into the region where $k \neq 0$ without traversing intermediate fields. For example, for electrostatic quadrupoles, this violates conservation of energy as the potential energy is thereby incremented without changing the kinetic energy (in magnetic quadrupoles, angular momentum conservation is violated).

The beamline designer may have learned that the third order aberrations calculated without fringe fields are incorrect, but he/she is still left with the impression that the fringe field is at fault and customizing it in some way will improve the third order optics. Further, of quadrupoles with the same effective length, those with short fringe fields are erroneously thought to be superior even though this often means they have smaller aperture. In fact, such quadrupoles are inferior, as their fifth order aberrations are worse: it can be shown that in the hard-edge limit, fifth order aberrations are singular [3].

ANALYTIC QUAD

A technique for finding the potential in all space given only the strength function $k(z)$ is given by Derevjankin [4, this reference is in Russian, but referred to by Vasil’ev [5]]:

$$V(x, y, z) = -\Re \left\{ \int_{z+iy}^{z+ix} dt \int_0^t k(\zeta) d\zeta \right\} \quad (2)$$

A particularly simple case that is realistic for short quads is

$$k(z) = \frac{K}{2} \text{sech}^2 z. \quad (3)$$

We find:

$$V = \frac{K}{2} \Re \{ -\log[\cos(x - iz)] + \log[\cos(y - iz)] \}. \quad (4)$$

See Fig. 1 where equipotential contours are plotted using as scaling potential $V_0 \equiv V(\frac{\pi}{4}, 0, 0) = \frac{K}{4} \log 2$. The transverse fields are locally nonlinear; at $z = 0$, $F_x \propto \tan x$, $F_y \propto \tan y$. Nevertheless, the integral of the transverse field is exactly linear:

$$\int_{-\infty}^{\infty} F_x dz = Kx, \quad (5)$$

and similarly, $\int F_y dz = -Ky$. The reason for this behaviour is that farther from axis, the transverse field is

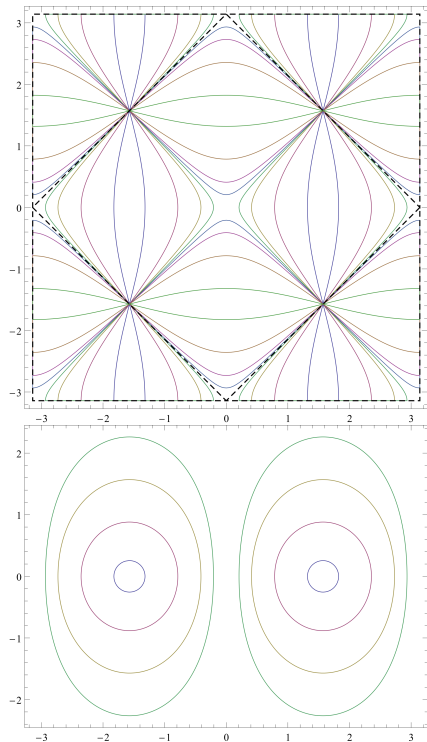


Figure 1: Equipotentials of Eq. 4. Upper: in $z = 0$ plane, contours $V = 4V_0$ (blue), $V = V_0$ (purple), $V = \frac{V_0}{4}$ (beige), $V = \frac{V_0}{16}$ (green), $V = -\frac{V_0}{16}$ (blue), $V = -\frac{V_0}{4}$ (purple), $V = -V_0$ (beige), $V = -4V_0$ (green). Lower: in $y = 0$ plane, contours $V = 4V_0$ (blue), $V = V_0$ (purple), $V = \frac{V_0}{4}$ (beige), $V = \frac{V_0}{16}$ (green).

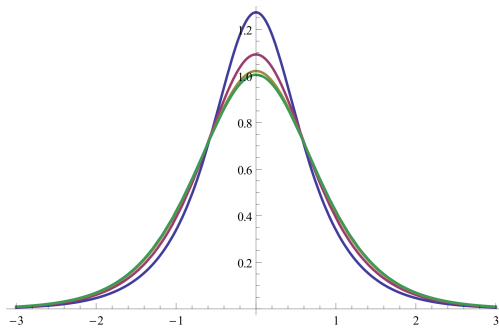


Figure 2: F_x/x vs. z for $x = \pi/4$ (blue), 0.5 (purple), 0.25 (brown), 0.125 (green).

stronger at $z = 0$, but weaker at the tails (it's 'peakier'). This is clarified in Fig. 2.

Integrated linearity from a locally nonlinear quad is not a surprise: from the symmetry and Laplace's equation, it can be shown that the following expansion holds:

$$V(x, y, z) = \frac{k}{2}(x^2 - y^2) - \frac{k''}{24}(x^4 - y^4) + \dots \quad (6)$$

Taking derivatives to find the fields, and integrating for constant x, y , we see that Eq. 5 holds for any choice of $k(z)$.

ISBN 978-3-95450-138-0

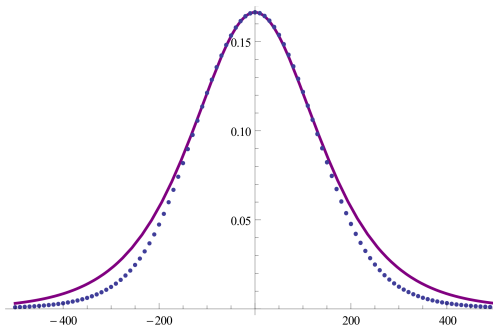


Figure 3: Magnetic field of the 12Q12 quadrupole (dots), measured at radius of 150 mm in the median plane vs. z in mm. The 12Q12 aperture radius is 155.6 mm, thus, $\sqrt{2}x = \sqrt{2}y = \frac{\pi}{4} \frac{150}{155.6}$. The continuous curve is the magnetic field at this same radius using Eq. 4, normalized to agree at $z = 0$.

EXAMPLE QUADRUPOLES

The potential V of the sech^2 quadrupole is periodic with period π in the x and y directions. At large z , the cancellation of this grid of alternating sign potentials ensures the rapid exponential falloff of the field. This is somewhat realistic. In the case of electrostatic quadrupoles, the ground planes dashed in Fig. 1 can be thought of as some approximation of the beam pipe. In magnetic quadrupoles the yoke takes the place of the ground surfaces. The yoke's proximity to the pole faces results in a characteristically quicker falloff as can be seen in Fig. 3, where the ideal sech^2 quadrupole is compared with a real quadrupole, namely, the TRIUMF 12Q12 (more on this quadrupole below).

Four choices of equipotential surfaces are shown in Fig. 4, oriented so that the quadrupole axis is vertical. Note the top left case is most like a long conventional quadrupole; the most significant difference being that the inside diameter varies along its length, as indicated by the $V = \pm \frac{V_0}{16}$ curves in the plot of Fig. 1. The lower right case in Fig. 4 would not give the correct fields without the 4 ground planes as the boundaries given by the 4 slender rods alone are insufficient. But the longer quadrupole (upper left in Fig. 4) case would work quite accurately without the ground planes.

As will be shown, this design has smaller aberrations than conventional designs, i.e. poles having constant xy cross section, truncated at each end. The only disadvantage is that the shape is rather more difficult to fabricate, having curvature on all directions.

Short Quadrupole Shapes

In the lower left of Fig. 4 (where the surfaces are strikingly similar in shape to four American regulation footballs) the potential of the shown surfaces is $\pm V_0$ and the curvature of the pole in the longitudinal direction is the same as in the transverse direction. This is an attractive feature because it allows as a good approximation for the pole to be symmetric along its axis, terminating in a spher-

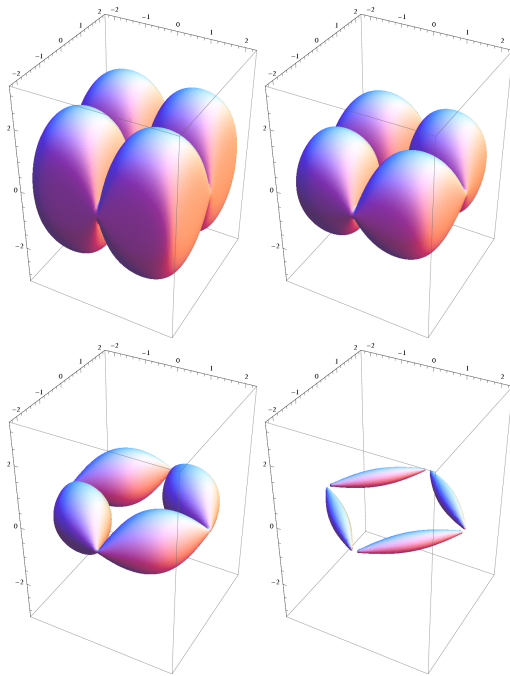


Figure 4: The coloured surfaces are 4 sets of equipotential surfaces of the potential (4). The quadrupole axis is vertical. In each case, the sides of the “box” containing the axes are also the 4 ground planes. All 4 give identical fields and the same sech^2 on-axis strength function if they are given the following potentials (left to right, top and then bottom), $\pm V_0/16, \pm V_0/4, \pm V_0, \pm 4V_0$ (adjacent surfaces have opposite sign).

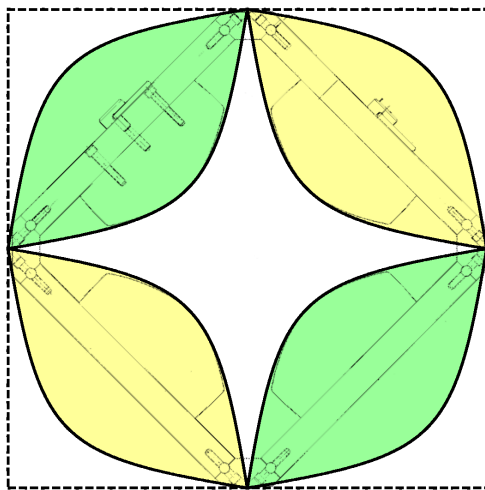


Figure 5: Cross section at $z = 0$ of the theoretical ideal sech^2 quadrupole (yellow and green) compared with drawing of the TRIUMF 12Q12 superposed. The yellow and green poles are circular in the orthogonal cross section, and hence shaped very much like the American football. The outer dashed square is at “ground” potential. Of the 12Q12 quadrupole, only the poles and the yoke are shown; coils are omitted. The black dot right of centre is the location of the Hall probe for measurements of Fig. 3.

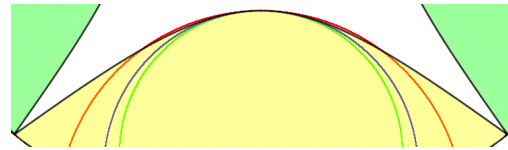


Figure 6: The “football” electrode with superposed, the circular arc of radius 1.15 times the aperture radius (green), $4/\pi$ (1.27) times the aperture radius (blue), and 1.54 times the aperture radius (red).

ical shape. What is the pole curvature that achieves this?

As the xy cross section is nearly hyperbolic, while the xz cross section is nearly a circle, it is clear that choosing a hyperboloid of revolution as shape is no better than choosing a spherical shape. The latter has the advantage that it is simpler to specify to the machinist.

As evident in the comparison in Fig. 5, the shape used for practicality, namely cylindrical poles terminating in a spherical pole-face, omits important parts of the “football” (the triangular regions either side of the poles in Fig. 5). This will have two effects: the quadrupole strength function $k(z)$ will not precisely follow a sech^2 law, and there will be some integrated 12-pole. The former is of little consequence, but the latter can cause aberration. However, just as with the case of the 2D quadrupole, we can alter the radius of curvature of the pole face to compensate the 12-pole. (20-pole and higher are not of course compensated in this technique but made slightly worse.)

In order to find the curvature radius that zeroes out the integrated 12-pole, Laplace’s equation was solved for a 3D boundary model, using OPERA. I am indebted to Chris Philpott of Buckley Systems Ltd. (New Zealand) for performing the final optimization [6].

The result found is that the radius of curvature in units of the aperture radius is 1.54 ± 0.01 :

$$\text{spherical pole-tip radius} = 1.54 \times (\text{aperture radius}). \quad (7)$$

The uncertainty arises from the grid coarseness and also from the variation due to surfaces “behind” the pole; surfaces which the engineer would be free to optimize for practicality. The potential on these surfaces also depends upon the insulator design in the case of electrostatic quadrupoles and the coil layout in the magnetic case.

This curvature is shown as the red curve in Fig. 6: one observes that it bulges past the “football” curve slightly on either side of centre. The blue curve is seen to properly match the “football” curve at the centre, and the green curvature, which is commonly used for such quadrupoles, is seen to not match the desired curvature at all. Reminder: the curvature of the ideal football shape in the direction orthogonal to the plane of the figure is essentially the blue curve.

The “12Q12” design

In the past, the short quadrupoles that have used rounded poles have used curvatures that are too sharp and as a result

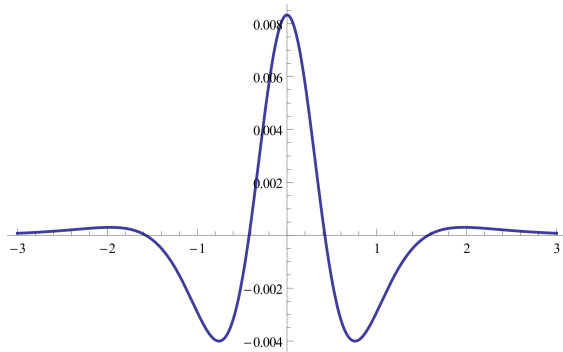


Figure 7: Fourth derivative of $k = \text{sech}^2(z)$.

the 12-pole does not integrate to zero. See Reeve et al. [7]. Of course, the point harmonic $A_6(z)$ is not zero, but $\propto k''''(z)$ even for the ideal pure quadrupole case. See Fig. 7 for $k = \text{sech}^2(z)$. What is found in actuality is for example Fig. 11 of Reeve et al. (1976) [7]: the 12-pole looks like Fig. 7 on top of a nonzero background that is due to the incorrect pole curvature.

Recently, quadrupoles of the design “12Q12/1.5” were constructed by Scanditronix Magnet AB [8] for TRIUMF [9]. Their integrated multipole components were measured, also by Scanditronix, using a rotating coil. These magnets’ radius of curvature near the pole centre is 1.14 times the aperture radius, which is too small by a factor 1.35, but this was partially offset by using a hyperboloid rather than a spherical shape. The 12-pole component was found to be roughly 20 times larger than the other multipoles: 0.0032 times the quadrupole field, at a radius of 94 mm, where the aperture radius is 155.6 mm.

Long Quadrupole Example

The aim of this example is to demonstrate that the conventional design quadrupole with a “tophat”-shaped strength function, has higher aberrations than the sech^2 quadrupole. Sech^2 quadrupoles need not be short. Refer to the $V = \pm \frac{V_0}{16}$ equipotentials in Fig. 1 to observe the shape of a long sech^2 quadrupole. The main difference in comparison with conventional quads is that the strength varies continuously along the quad. One method of obtaining this is to flare the aperture, varying it continuously from centre outward. Admittedly, this complicates the design and would increase the construction cost, especially for superconducting quads.

For illustration, we take as an extreme example the CERN LHC β^* quadrupoles. We take as round figures, a length of 6 m, aperture radius of 35 mm, gradient of 200 T/m, and use the Enge coefficients of the “LHCHGQ” [10]. We construct a model sech^2 quadrupole of the same integrated strength (1200 T), and same integrated squared strength of 240,000 T²/m. This latter ensures that the third order aberrations are the same [2]. The Sech^2 strength function scaled to satisfy these two integrals

ISBN 978-3-95450-138-0

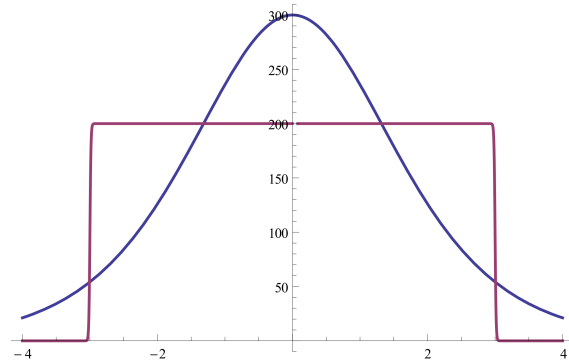


Figure 8: Gradient (in T/m) vs. z (in m) for the CERN LHC IP quadrupole (purple), compared with a sech^2 strength quadrupole of the same aperture (blue). Note that the latter quad would be impractical on two counts: its field extends outside the 6 m space allotted in the LHC, and it would need to be 1.5 times stronger at its peak. The comparison is only to illustrate that quads with optimally soft fringe fields have lower fifth and higher order aberrations.

is

$$k(z) = \left(300 \frac{\text{T}}{\text{m}}\right) \text{sech}^2\left(\frac{z}{2 \text{ m}}\right) \quad (8)$$

Using COSY- ∞ [11] and a proton energy of 7 TeV, we compared the aberrations to seventh order; these are shown in Table 1. (For the LHCHGQ, we had to modify slightly the COSY- ∞ routine FFELE as the fringe field given in ref. [10] has an anomalously large extent). For the implementation of the sech^2 quadrupole in COSY- ∞ , see Ref. [1].

As expected, the third order aberrations are the same for the two types. The thin lens formula for the aberrations is [2]:

$$\Delta x' = \frac{\int k^2 dz}{(B\rho)^2} \left(-\frac{1}{3}x^3 - xy^2\right) \quad (9)$$

$$= -\frac{0.000147}{\text{m}^3}x^3 - \frac{0.000440}{\text{m}^3}xy^2$$

$$\Delta y' = \frac{\int k^2 dz}{(B\rho)^2} \left(-x^2y - \frac{1}{3}y^3\right) \quad (10)$$

$$= -\frac{0.000440}{\text{m}^3}x^2y - \frac{0.000147}{\text{m}^3}y^3$$

These agree well with the values in Table 1, when the thick lens effect is taken into account. (This reduces the aberration effect in the focusing direction and exacerbates in the defocusing direction.)

But at higher than third order, the aberrations are not at all the same. The fifth order aberrations are about 200 times smaller for the sech^2 quadrupole, and the largest seventh order coefficients are roughly 100,000 times smaller for the sech^2 quadrupole. For ninth order, the ratio is 10^8 .

It is doubtful that a superconducting quadrupole with Eq. 8 as strength function is at all feasible, and in any case would be too long to fit into the interaction region of the LHC. Further, there is nothing to suggest that the

LHCHGQ quad	sech ² quad	
$\Delta x'$ or $\Delta y'$	$\Delta x'$ or $\Delta y'$	mn
-0.4877909E-01	-0.4879330E-01	10
0.5406070E-01	0.5407527E-01	01
-0.1154336E-03	-0.1134717E-03	30
-0.3724576E-03	-0.4038506E-03	21
-0.4881636E-03	-0.4714397E-03	12
-0.1822114E-03	-0.1867242E-03	03
0.1017362E-02	-0.2979146E-05	50
-0.7305652E-02	-0.1326917E-04	41
0.4749991E-02	-0.2637724E-04	32
-0.7580379E-02	-0.3096770E-04	23
0.2348281E-02	-0.1566155E-04	14
-0.8101367E-03	-0.3084560E-05	05
-0.1109434	-0.1215269E-06	70
0.9689789	-0.6573820E-06	61
-0.7151169	-0.1949172E-05	52
1.312496	-0.2858019E-05	43
-0.2433022	-0.2866705E-05	34
0.5811675E-02	-0.2532962E-05	25
0.6676453	-0.8507323E-06	16
-0.1404954	-0.1333598E-06	07

Table 1: Aberration coefficients of the LHC “high gradient quadrupole”, compared with quadrupole of sech² strength function. m and n are the exponents of x and y ; for example, the fourth line is the coefficients for x^2y .

aberrations calculated for the LHCHGQ quads in any way limit the performance of the LHC. However, this comparative study puts to rest the notion that quadrupoles with smoothly varying strength function, being in a sense “all fringe field” [7], are optically inferior to more conventional quadrupoles with harder edges. In fact, quite the opposite is true.

The $k(z) \propto \text{sech}^2 z/D$ case is not special; any smoothly varying k would have similar low aberration properties. The advantage of the sech² case is that there is a handy, simple expression for the potential, and at least in the case of very short quads, this expression is a good approximation.

Thus our results can be understood as follows. In the traditional design, the poles terminate abruptly, and this results in aberrations that scale with the ratio of beam size to aperture, raised to a power appropriate for the order of the aberration. In the case of the design proposed here, the aberrations scale with the ratio of beam size to quadrupole length, raised to that same power.

CONCLUSIONS

We have derived an analytic potential for quadrupoles, both long and short. The strength function, instead of stepping up abruptly at the entrance and down at the exit, varies smoothly throughout the quadrupole. We have shown that this results in lower field aberrations.

REFERENCES

- [1] R. Baartman, “Quadrupole shapes,” *Phys Rev Special Topics Accelerators and Beams*, vol. 15, no. 7, p. 74002, 2012.
- [2] R. Baartman, “Intrinsic third order aberrations in electrostatic and magnetic quadrupoles,” in *Particle Accelerator Conference, 1997. Proceedings of the 1997*, vol. 2, pp. 1415–1417, IEEE, 1997.
- [3] A. Dragt, April 1999. private communication.
- [4] G. Derevjankin, “On the representation of the quadrupole lens potential,” *Zh. Tkh. Fiz. (USSR)*, vol. 42, no. 6, pp. 1178–1181, 1972.
- [5] G. Vasil’ev, “Spatial field of a quadrupole lens: An analytical approach,” *Nuclear Instruments and Methods*, vol. 151, no. 1-2, pp. 65–68, 1978.
- [6] C. Philpott, September 2012. private communication.
- [7] P. Reeve, T. Gathright, and R. Fyvie, “Quadrupole magnet field measuring equipment at triumf,” *Nuclear Instruments and Methods*, vol. 135, no. 3, pp. 459–472, 1976.
- [8] tech. rep., Scanditronix Magnet, 2010. Newsletter.
- [9] G. Morris, Sept 2011. private communication.
- [10] M. Berz, B. Erdélyi, and K. Makino, “Fringe field effects in small rings of large acceptance,” *Physical Review Special Topics-Accelerators and Beams*, vol. 3, no. 12, p. 124001, 2000.
- [11] M. Berz, “Computational aspects of optics design and simulation: Cosy infinity,” *Nuclear Instruments and Methods in Physics Research Section A: Accelerators, Spectrometers, Detectors and Associated Equipment*, vol. 298, no. 1-3, pp. 473–479, 1990.